

Hyperspectral Imaging for Skin Cancer Diagnosis in Mice

Tsapras Athanasios

Department of Electronics and Computer Engineering, Technical University of Crete, Chania, Crete, Greece

Introduction

Melanoma is a malignant transformation of pigment-producing cells (melanocytes) that are mostly located in the skin and arise from the differentiation of neural crest progenitor cells during embryonic development. The incidence of melanoma has risen sharply in the last 4 decades and the death rate from it has doubled in the last 35 years malignant melanoma of the skin accounts for 160,000 new cases of cancer annually [1]. *In vivo*, early detection of pre-malignant lesions is crucial for melanoma prevention. A prerequisite for establishing more reliable diagnostic criteria is the better understanding of melanoma development processes. The objective of the study was the development of a melanoma animal model and the monitoring of the melanoma development processes, with the aid of HIS [2], attempting to establish more reliable criteria in discriminating dysplastic nevi from melanomas.

Materials and Methods

Melanoma development was induced on 14 mice treated with a chemical carcinogen. The study lasted about 18 months and took place in three phases:

A) *Animal Model*. Melanoma induction on 14 newborn mice were obtained following a DMBA, Croton oil chemical carcinogenesis protocol in C57Bl mice and in animals of the same genetic background harboring a deletion in the Tpl2 protooncogene. Previous studies revealed that Tpl2 activates the ERK, JNK and p38 MAPK pathways. Deletion of Tpl2 blocked ERK1 and ERK2 activation and was linked to defects in production of Tumor Necrosis Factor- α (TNF- α) [3-6]. The link of BRAF to melanoma as an activator of a branch of MAPK pathway and the frequent context-dependent association of many oncogenes, justified testing the Tpl2 knockouts as potential models for the induction of melanomas.



Figure 1: The Hyperspectral Imaging System (HIS)

B) *Hyperspectral Imaging*. All mice were monitored using the HIS which is illustrated in Figure 1. The system is capable of acquiring spectral images of 10 nm full width half maximum (FWHM), with 3 nm tuning step, in the spectral range 400–1000 nm. The minimum transmittance is 40% across its operational spectral range [7,8]. The use of IEEE-1394 data transfer protocol provides the possibility of acquiring images at a rate of 15 frames/s at full resolution and of more than 30 frames/s at VGA resolution. Thus, for each mouse, a 30 band spectral cube was acquired. From each spectral cube, a full spectrum for every image pixel was calculated.

Spectra were analyzed using the Spectral Angle Mapper (SAM) algorithm. SAM measures the spectral similarity by calculating the angle between two spectra (image and reference spectrum) (Figure 2), treating them as vectors in n-dimensional space:

$$a = \cos^{-1} \left(\frac{\sum_{i=1}^{nb} t_i r_i}{\left(\sum_{i=1}^{nb} t_i^2 \right)^{1/2} \left(\sum_{i=1}^{nb} r_i^2 \right)^{1/2}} \right), \quad (1)$$

where n_b = the number of bands, t_i = the test spectrum and r_i = the reference spectrum.

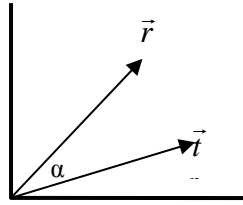


Figure 2: The Spectral Angle Mapper calculates the Spectral Angle between the test spectrum (t) and the reference one (r).

Small angles between the two vectors (spectra) indicate high similarity, whereas greater angles indicate lower similarity [9]. Spectral similarities produce a pseudocolor map whose colors represent degrees of variations in the tissue spectral characteristics associated with the progress of the disease (Figure 3).

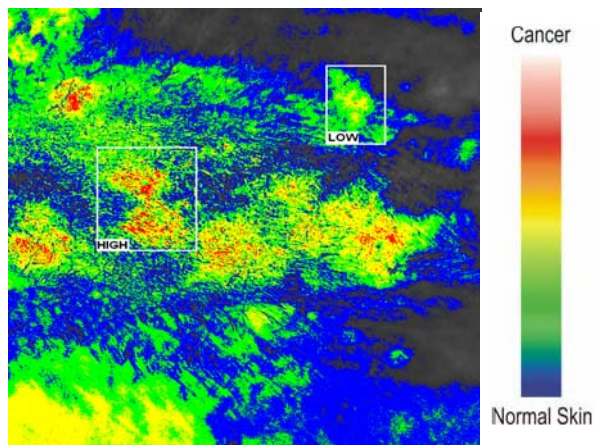


Figure 3: Pseudocolor map pointing the obtained biopsy samples. The map's colors represent degrees of variations in the tissue spectral characteristics associated with the progress of the disease.

C) Histology. Using the pseudocolor map as a guide, biopsy samples were obtained from areas with altered spectral characteristics (indicated as high-grade lesions) and from normal tissue areas. In total, 26 biopsy samples were collected and submitted for histological evaluation (Table 1).

Table 1: Genotype/sex, prediction of the study and diagnosis (biopsy), per mouse.

Mouse #	Genotype/Age/Sex	Diagnosis	
		HG prediction	LG prediction
1	KO/15m/F	melanoma	melanoma
2	KO/15m/F	melanoma	normal
3	KO/15m/F	melanoma	normal
4	KO/15m/F	melanoma	normal
5	KO/12m/F	melanoma	normal
6	KO/12m/F	melanoma	melanoma
7	KO/12m/F	melanoma	melanoma
8	KO/12m/F	normal	normal
9	KO/12m/F	melanoma	normal
10	WT/12m/M		normal
11	WT/12m/M	neoplasm	
12	WT/12m/M	normal	normal
13	WT/12m/F	normal	normal
14	WT/12m/M	melanoma	normal

Results

DMBA treatment effectively induced melanomas in 100% of the Tpl-2 knockouts versus 30% of the wild-type mice. The sensitivity and specificity of HIS in discriminating melanomas from dysplastic nevi were both found to be 77%.

Table 2: Sensitivity and specificity of the method

	BIOPSY	
	TRUE	FALSE
PSEUDO COLOR MAP		
POSITIVES	10	3
NEGATIVES	10	3

Conclusions

The obtained results indicate that the combination of HIS and SAM algorithm is capable of differentiating dysplastic nevi from melanomas objectively and with high accuracy. This approach exhibits the potential for the development of a screening platform that would allow the *in vivo* non-invasive detection and grading of skin malignancies in mice, thus facilitating the utilization of the mouse model in the study of melanoma induction and experimental therapies. This technology could provide a valuable tool for the evaluation of treatment modalities and holds the promise to provide a cost-effective screening technology for early detecting precancerous lesions of human skin.

References

1. DM Parkin, F. Bray, J. Ferlay and P. Pisani (2005) Global cancer statistics, 2002, CA Cancer J Clin 55: 74-108.
2. CD Dumitru, JD Ceci, C. Tsatsanis, D. Kontoyiannis, K. Stamatakis, JH Lin, C. Patriotis, NA Jenkins, NG Copeland, G. Kollias and PN. Tsihchlis (2000) TNF-alpha induction by LPS is regulated posttranscriptionally via a Tpl2/ERK-dependent pathway, Cell. 103(7):1071-83.
3. C. Balas (2001) A novel optical imaging method for the early detection, quantitative grading, and mapping of cancerous and precancerous lesions of cervix, IEEE Trans Biomed Eng 48: 96-104.
4. C. Patriotis, A. Makris, SE Bear and PN Tsihchlis (1993) Tumor progression locus 2 (Tpl-2) encodes a protein kinase involved in the progression of rodent T-cell lymphomas and in T-cell activation, Proc Natl Acad Sci U S A 90: 2251-5.
5. C. Patriotis, A. Makris, J. Chernoff and PN. Tsihchlis (1994) Tpl-2 acts in concert with Ras and Raf-1 to activate mitogen-activated protein kinase, Proc Natl Acad Sci U S A 91: 9755-9.
6. C. Patriotis, MG Russeva, JH Lin, SM Srinivasula, DZ Markova, C. Tsatsanis, A. Makris, ES Alnemri and PN. Tsihchlis (2001) Tpl-2 induces apoptosis by promoting the assembly of protein complexes that contain caspase-9, the adapter protein Tvl-1, and procaspase-3, J Cell Physiol 187: 176-87.
7. N. Katzilakis, E. Stiakaki, A. Papadakis, H. Dimitriou, E. Stathopoulos, E. Markaki, C. Balas and M. Kalmanti (2004) Spectral characteristics of acute lymphoblastic leukemia in childhood, Leukemia Research 28:1159-1164.
8. A. Papadakis, E. Stathopoulos, G. Delides, K. Berberides, G. Nikiforidis and C. Balas (2003) A Novel Spectral Microscope System: Application in Quantitative Pathology, IEEE Trans Biomed Eng 50(2): 207-217.
9. G. Girouard, A. Bannari, A. El Harti and A. Desrochers (2004) Validated Spectral Angle Mapper Algorithm for Geological Mapping: Comparative Study between Quickbird and Landsat-TM, Geo-Imagery Bridging Continents, Istanbul, 599-604.